Hyperfine sublevel correlation spectroscopy in lithium silicate glasses

L. Astrakas, Y. Deligiannakis, G. Mitrikas, and George Kordas

Citation: The Journal of Chemical Physics **109**, 8612 (1998); doi: 10.1063/1.477527
View online: http://dx.doi.org/10.1063/1.477527
View Table of Contents: http://scitation.aip.org/content/aip/journal/jcp/109/19?ver=pdfcov
Published by the AIP Publishing

Hyperfine sublevel correlation spectroscopy in lithium silicate glasses

L. Astrakas, Y. Deligiannakis, G. Mitrikas, and George Kordas
Institute of Materials Science, National Center for Scientific Research Demokritos, 15310 Aghia Paraskevi Attikis, Greece

(Received 30 June 1998; accepted 11 August 1998)

The structure of γ-irradiated $(Li_2O)_{0.1}(SiO_2)_{0.9}$ glass has been studied with two-dimensional hyperfine sublevel correlation spectroscopy (HYSCORE). The theoretical evaluation of the HYSCORE experimental data revealed the existence of weak couplings between the electron spin and nearby Li. The anisotropic hyperfine coupling T is equal to 4.0 MHz suggesting a nonbridging oxygen—Li distance of 2.0 Å and an angle of $\pm 60°$ away from the g_z axis. The A_{iso} value is equal to 0.5 MHz, corresponding to 0.135% contribution of the Li $2s$ orbital to the ground state. Thus, an estimation can be made of the covalent character of the bond between the nonbridging oxygen and the alkali. © *1998 American Institute of Physics.* [S0021-9606(98)51343-8]

I. INTRODUCTION

Two-dimensional hyperfine sublevel correlation spectroscopy (HYSCORE)[1] is a four-pulse electron spin echo envelope modulation (ESEEM) technique,[2] analogous to homonuclear correlation spectroscopy (COSY) NMR spectroscopy.[3] ESEEM techniques are suitable for resolving weak magnetic interactions between paramagnetic centers and nearby nuclei. These couplings are usually unresolved in continuous wave electron paramagnetic resonance (EPR) experiments due to the inhomogeneous broadening. In the case of many overlapping nuclear transition frequencies, the interpretation of the one-dimensionalESEEM spectra becomes difficult. This happens when more than one type of nuclei surround the paramagnetic center or for $I > I/2$. An additional difficulty arises when the sample is amorphous and has large anisotropic hyperfine interactions that produce spectral features which are braodened and deformed. In such cases HYSCORE is a promising technique for the proper assignment of the various couplings.

So far, HYSCORE has been applied in biological as well as in inorganic materials.[4–15] For example, using HYSCORE, the hyperfine interaction parameters have been determined for:

(a) nitrogens in pheophytine anion radical in Photosystem II,[9]
(b) coordinating nitrogens in oxovanadium complexes,[11–13]
(c) nitrogens surrounding iron–sulfur centers,[8]
(d) aluminum nuclei around anthraquinone molecules,[14] and
(e) protons in transition metal ion complexes.[15]

In the present paper, we studied a $(Li_2O)_{0.1}(SiO_2)_{0.9}$ glass that becomes paramagnetic after γ irradiation. The cw-EPR spectroscopy showed that two centers contribute to the signal in silicate glasses related to nonbridging oxygens (NBOs).[16–20] The relative concentration of the centers depends on the alkali metal concentration.[20] Specifically, the one ($H_{\perp}$ center) was assigned to a hole trapped at one NBO and the other ($H_{\parallel}$ center) was attributed to a hole trapped between two NBOs.[16,20] In our glass, the $H_{\perp}$ center dominates the cw-EPR spectrum.[20] The models proposed for the structure of the $H_{\perp}$ center in literature[17–20] are inexact regarding the NBO–Li distance and Si–NBO–Li angle. This arises from the low resolution of cw-EPR techniques.[9–12] Here, we outline the ability of HYSCORE to unravel various weak couplings and deduce detailed structural information about the $(Li_2O)_{0.1}(SiO_2)_{0.9}$ glass.

II. EXPERIMENT

$(Li_2O)_{0.1}(SiO_2)_{0.9}$ glass has been prepared by the melting technique. Batches of 30 g were put in an alumina crucible at 1650 °C for 6 h, followed by rapid quenching in water. The amorphous state was confirmed by x-ray diffraction analysis and the stoichiometry was confirmed by an ICP Optima 3000 spectrometer. Finally the sample was irradiated with a ^{60}Co source. For the EPR experiments, a Bruker ESP 380 spectrometer was used equipped with a dielectric resonator. The duration of the $\pi/2$ and π pulses was 16 and 32 ns, respectively, with equal amplitudes. To remove the unwanted echoes, the appropriate phase-cycling procedures were applied.[21,22] The background decay in both t_1 and t_2 dimensions was subtracted using a linear function followed by zero filling to 512 points in two dimensions and by tapering with a Hamming window; then Fourier transform was carried out in both dimensions.

III. RESULTS

A. Measurements of spectra

The HYSCORE experiment (Fig. 1), consists of four microwave ($\pi/2$-τ-$\pi/2$-t_1-π-t_2-$\pi/2$)pulses. The first two $\pi/2$ pulses are separated by the preparation interval τ and create the nuclear coherences.[4] After the evolution interval t_1, a mixing π pulse exchanges the populations of the m_s manifolds creating correlations between the corresponding nuclear transitions. Finally, after the detection interval t_2, a third $\pi/2$ pulse creates the electron spin echo.

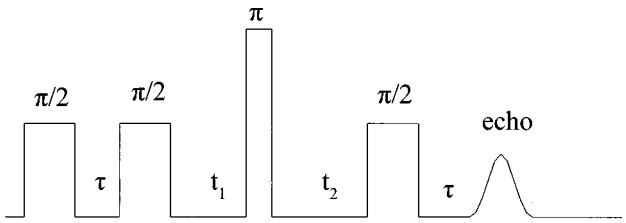

FIG. 1. Pulse sequence of HYSCORE experiment.

In order to avoid suppression effects,[7] a series of HYSCORE spectra were recorded at different tau values. Figures 2(A), 2(B), and 2(C) show HYSCORE spectra recorded for $(Li_2O)_{0.1}(SiO_2)_{0.9}$ glass for τ=128, 224, and 352 ns, respectively. It is easy to distinguish the two Li isotope cross peaks because their Larmor frequencies (2.16 MHz for ^{6}Li and 5.71 MHz for ^{7}Li) are far enough. So we can consider that cross peaks in the vicinity of a given Larmor frequency belong to the corresponding Li isotope. At τ=128 ns [Fig. 2(A)], two broad features around the ^{7}Li Larmor frequency together with two other pairs of cross peaks, with coordinates (16.2, 4.2 MHz) and (17.5, 6.7 MHz) are resolved. In addition a ridge normal to the diagonal at the ^{6}Li Larmor frequency is observed. At the (+,−) quadrant a pair of cross peaks exist with coordinates (4, −8 MHz). Finally, some peaks close to the frequency axis are observed, but their real importance is doubtful since they are very sensitive to the windowing. At τ=224 ns [Fig. 2(B)], we have the same ridge as in Fig. 2(A) near the ^{6}Li Larmor frequency. There is a bump around the ^{7}Li Larmor frequency and two pairs of cross peaks around it, with coordinates (8, 4 MHz) and (2.2, 9.7 MHz). Also, we observe two more cross peaks around (12.5, 5.5 MHz) and (10.3, 6.7 MHz). At the (+,−) quadrant there are two cross peaks with coordinates ±(2.6, −5.7 MHz). At τ=352 s [Fig. 2(C)], a pair of cross peaks at (1, 3.5 MHz), marked with a dashed line is resolved.

B. Simulation of spectra

For $I=1/2$ and small anisotropy hyperfine interaction, the assignment of the HYSCORE spectrum is rather simple.[1,6,9] For $A_{iso}<2\upsilon_I$the cross peaks have coordinates $(\upsilon_I+A_{iso}/2,\upsilon_I-A_{iso}/2)$, they appear at the (+,+) quadrant, and their frequency distance is a direct measurement of A_{iso}. The anisotropic hyperfine coupling T, is related to the extent of the peaks.[6] For $A_{iso}>2\upsilon_I$ the peaks are at coordinates $(A_{iso}/2+\upsilon_I, A_{iso}/2-\upsilon_I)$ with maximum intensity at the (+,−) quadrant. For $I>1/2$(^{6}Li has $I=1$ and ^{7}Li has $I=3/2$) many peaks are expected and probably they contribute to both quadrants.[14] In such cases, the exact assignment requires numerical simulations, otherwise it is not safe to conclude whether two neighboring peaks belong to different couplings or if they are part of the same, suppressed ridge.

Neglecting the relaxation effects, the echo intensity is expressed as[5]

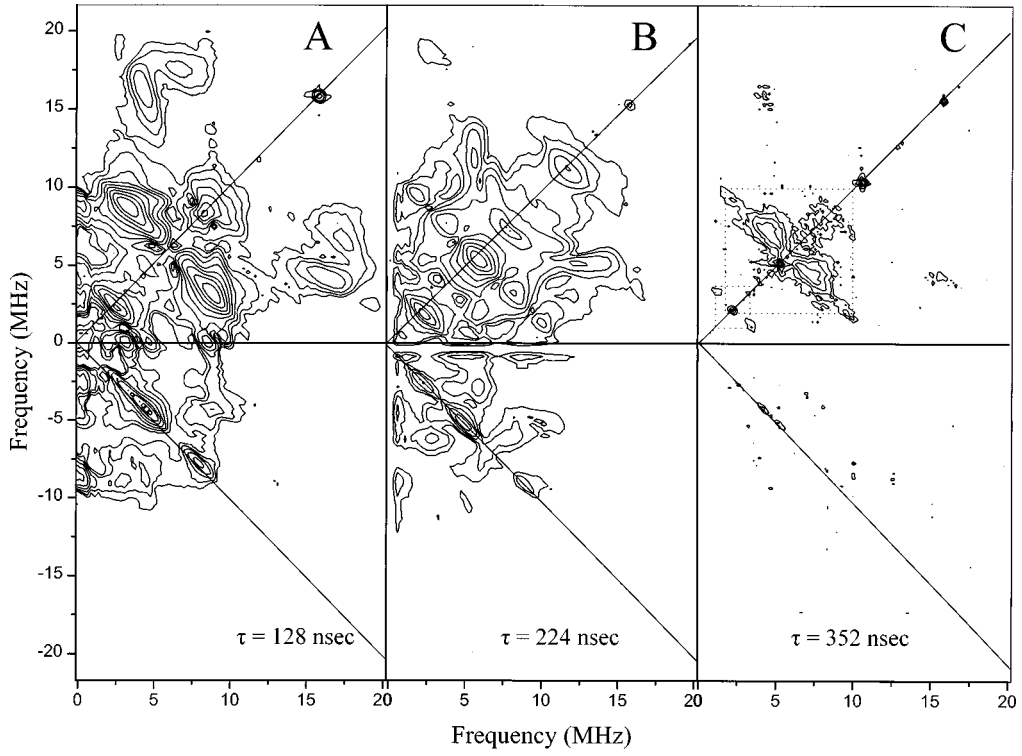

FIG. 2. Experimental 2D-HYSCORE spectrum (contour plots) of $(Li_2O)_{0.1}(SiO_2)_{0.9}$ glass recorded at τ=128 ns (A), τ=224 ns (B), and τ=352 ns (C). Experimental conditions: $t_1\times t_2=128\times128$ points for (A) and 256×256 points for (B) and (C); start values $t_1=56$ ns, $t_2=56$ ns; microwave frequency, 9.70 GHz; magnetic field strength 3455 G; sample temperature 20 K; time interval between successive pulse sets, 3 ms; 20 events were averaged; temperature =20 K.

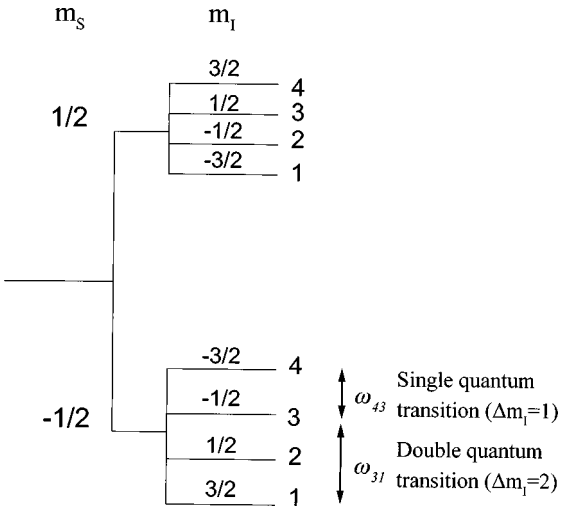

FIG. 3. Energy level at constant field for $S=1/2, I=3/2$.

$$E(\tau,t_1,t_2)=(1/(8I+4))\sum_{ij,kl}\{C^{a}_{ik\ \ln}(\tau)e^{-i\omega^{\alpha}_{ik}t_2}e^{-i\omega^{\beta}_{\ln}t_1}+C^{\beta}_{ik\ \ln}(\tau)e^{-i\omega^{\alpha}_{ik}t_1}e^{-i\omega^{\beta}_{\ln}t_2}\},\quad(1)$$

where

$$C^{a}_{ik\ \ln}(\tau)=\sum_{jm}(M_{il}M^{*}_{jl}M_{jn}M^{*}_{kn}M_{km}M^{*}_{im})\times(e^{-i(\omega^{\alpha}_{ij}+\omega^{\beta}_{lm})\tau}+e^{-i(\omega^{\alpha}_{kj}+\omega^{\beta}_{nm})\tau}),\quad(2)$$

$$C^{\beta}_{ik\ \ln}(\tau)=\sum_{jm}(M_{il}M^{*}_{jl}M_{jn}M^{*}_{kn}M_{km}M^{*}_{im})^{*}\times(e^{-i(\omega^{\alpha}_{ij}+\omega^{\beta}_{lm})\tau}+e^{-i(\omega^{\alpha}_{kj}+\omega^{\beta}_{nm})\tau}).\quad(3)$$

In the above expressions, M_{ij} is the EPR transition amplitude from the i sublevel within the α electron spin manifold to the j sublevel within the β manifold. $\omega_{ij}=\omega_i-\omega_j$ is the frequency of the nuclear transition between i and j nuclear sublevels within the same electron spin manifold (Fig. 3).

In the frequency domain, the two-dimensional spectrum contains peaks at frequencies $(\omega^{\alpha}_{ij},\omega^{\beta}_{lm})$ and $(\omega^{\beta}_{lm},\omega^{\alpha}_{ij})$ which are symmetric with respect to the diagonal. From the expression of the echo intensity [Eq. (1)] it is seen that the spectrum at the frequency domain is symmetric around the point (0,0), i.e., the peaks at $(\omega^{\alpha}_{ij},\omega^{\beta}_{lm})$and $(-\omega^{\alpha}_{ij},-\omega^{\beta}_{lm})$ have the same intensity, so only two quadrants [(+,+) and (+,−)] have to be considered.[4] In the case where considerable anisotropic hyperfine and quadrupole interactions are present then the peaks are elongated and become ridges.[6] The positions, the shapes, and the intensities of the various features are determined by the time interval τ and the size of the terms in the spin Hamiltonian. The spin Hamiltonian for an $S=1/2$ center interacting with a nucleus with nuclear spin quantum number I is[23]

$$H=\beta\mathbf{B}\cdot\mathbf{g}\cdot\mathbf{S}-g_n\beta_n\mathbf{B}\cdot\mathbf{I}+\mathbf{I}\cdot\mathbf{A}\cdot\mathbf{S}+\mathbf{I}\cdot\mathbf{Q}\cdot\mathbf{I}.\quad(4)$$

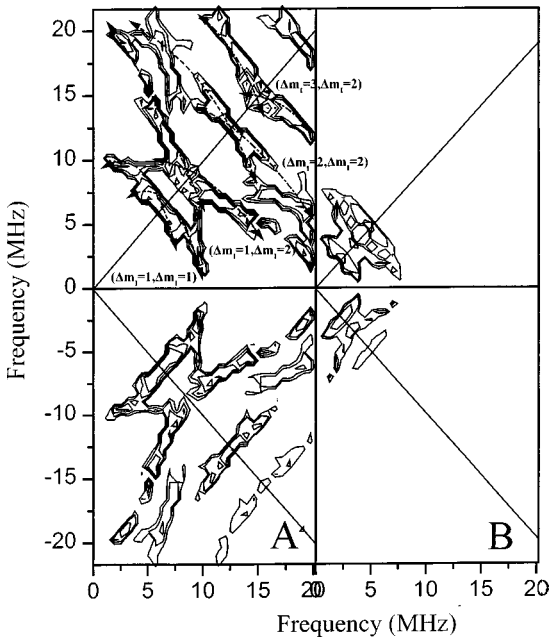

FIG. 4. Calculated HYSCORE spectrum of a ^{7}Li nucleus (A) and a ^{6}Li nucleus (B) for $\tau=224$ ns with parameters given in Table I ($t_1\times t_2=128\times128$ points). Orientation selection impose the constraint: $40°<\theta<140°$. Dashed lines mark the correlated nuclear transitions. The corresponding m_I changes are inserted in parenthesis.

The hyperfine tensor **A** has principal values (A_{xx},A_{yy},A_{zz}). In the point-dipole approximation it can be written in the form $(A_{\rm iso}-T,A_{\rm iso}-T,A_{\rm iso}+2T)$ where $A_{\rm iso}$ is the isotropic hyperfine coupling constant and $T=gg_n\beta_n\beta/hr^3$ where r is the effective electron–nucleus distance. Q is the nuclear quadrupole tensor; its components in its principal axes system are $Q^P_{zz}=Q/2I(2I-1)$, $Q^P_{xx}=-Q^P_{zz}(1-\eta)/2, Q^P_{yy}=-Q^P_{zz}(1+\eta)/2$, where $\eta=(Q^P_{xx}-Q^P_{yy})/Q^P_{zz}$ and $Q=e^2qQ_n/h$ is the quadrupole coupling constant due to a quadrupole moment Q_n, interacting with the electric field gradient q at the nucleus. The principal axes systems of the tensors **A** and **Q** are related by the Euler angles (α,β,γ).

The simulation can also verify whether peaks that appear on the diagonal [i.e., peaks at 7.7 and 11.7 MHz in Fig. 2(B)] correspond to existing couplings or if they are due to experimental artefacts.

Figure 4(A) is a representative simulation for one ^{7}Li nucleus for $\tau=224$ ns, the simulation parameters are listed in Table I. For ^{7}Li the quadrupole interaction is expected to be negligible, ($Q<0.2$ MHz) and thus its effect on the HYSCORE spectra can be practically ignored. From the simulation it is clear that many of the apparent individual, cross peaks in the HYSCORE spectrum of Fig. 2(B) belong

TABLE I. Calculated parameters for ^{7}Li and ^{6}Li couplings in $(Li_2O)_{0.1}(SiO_2)_{0.9}$ glass.

	^{7}Li	^{6}Li
$A_{\rm iso}$ (MHz)	0.5±0.1	0.2±0.05
T (MHz)	4±0.2	1.5±0.2
Q (MHz)	<0.2	~0
β (degrees)	60±20	60±20

to the same extended ridge due to the large anisotropy ($T=4$ MHz). The arrows in Fig. 4(A) mark the various nuclear transitions for $I=3/2$. We notice that in our case where the quadrupole term is small:

(1) peaks with the same Δm_I have the same positions, and
(2) usually the more intense peaks come from the transitions with smaller Δm_I.

These statements are valid for every nuclear spin I, under the condition that the quadrupole term can be neglected to first-order approximation. The first statement is based on the fact that the eigenvalues of the Hamiltonian (1) are proportional to the m_I.[24] The second statement can be justified if we extend the group-theoretical argument of Dikanov[2] for the three pulse ESEEM, to the HYSCORE case. According to this, the expression describing the HYSCORE spectrum for a nuclear spin $I>1/2$ is a polynomial of degree $2I$ of the corresponding expression for $I=1/2$.[2] For example the following expression for HYSCORE ($I=1/2$):[1]

$$E(t_1,t_2)\propto c^2\cos(\omega_b t_2+\omega_a t_1+\varphi)+\cdots \tag{5}$$

will be transformed for spin $I=3/2$ to

$$E(t_1,t_2)\propto -c^2\cos(\omega_b t_2+\omega_a t_1+\varphi)+\frac{c^6}{2}\cos(3\omega_b t_2+3\omega_a t_1+3\varphi)+\cdots . \tag{6}$$

Expression (3) is a third degree polynomial $(8x^3-4x)$ of expression (2).[25] Using the fact that $c^2>c^6/2$, (c^2 is a transition probability so $c^2<1$), from Eq. (3) it is clear that the peak (ω_a,ω_b) with $\Delta m_I=1$ will be more intense than the peak $(3\omega_a,3\omega_b)$ with $\Delta m_I=3$.

Hyperfine interactions of ^{6}Li and ^{7}Li are scaled according to their Larmor frequencies $(\nu_I(^6\mathrm{Li})/\nu_I(^7\mathrm{Li})=2.16/5.71)$. Accordingly the hyperfine parameters of ^{6}Li are calculated from the corresponding parameters of ^{7}Li and they are listed in Table I. The simulated spectrum for ^{6}Li is shown in Fig. 4(B) and reproduces well the corresponding part of the experimental spectrum of Fig. 2(B). The remaining broad features around the Li Larmor frequency are produced by weakly coupled ''matrix'' Li nuclei and the peak at (11.7, 11.7 MHz) corresponds to a ''double quantum'' $(\Delta m_I=2)$ nuclear transition of the matrix ^{7}Li nuclei [Fig. 2(B)].

IV. DISCUSSION

Our previews analysis showed that the ^{7}Li anisotropic hyperfine tensor is axial with value $T=4.0$ MHz. According to the point-dipole approximation ($T=g_e g_n \beta_e \beta_n / hr^3$), this value means that the effective distance between the electron spin and the alkali nucleus is 2.0 Å. This represents the distance between the nonbridging oxygen and the alkali and matches perfectly with the distance determined by the neutron diffraction and x-ray analysis of lithium silicate glasses.[26] Also, according to the point dipole approximation the z axis of the hyperfine tensor has the Li–O direction. Simple linear combination of localized orbitals-molecular orbital (LCLO-MO) calculations[27] showed that we can assume that the z principal axis of the g tensor has the Si–O direction. Assuming that the same is valid in our case and using our result, that the angle between z axis of hyperfine and g tensor is close to 60°, we present in Fig. 5 a working model of the local environment of the nonbridging oxygen. According to this the availability of nearly equivalent Li sites close to the nonbridging oxygen, as originally proposed by Charles,[28] is restricted within the dashed circle of Fig. 5. The small A_{iso} value also supported the model that the Li ion is located far from the high spin density lobes of oxygen's p_x or p_y orbitals.

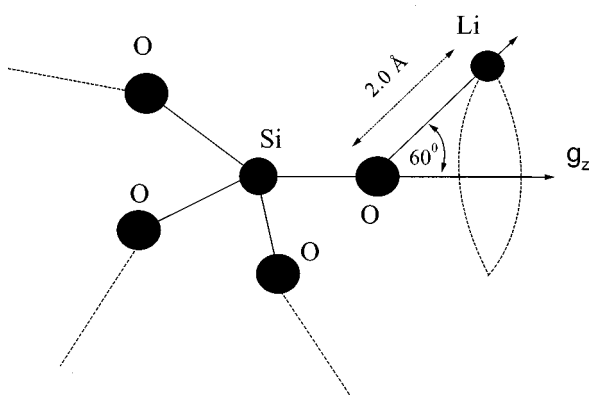

FIG. 5. Structural model for local environment of a nonbridging oxygen in $(Li_2O)_{0.1}(SiO_2)_{0.9}$ glass. Dashed circle shows equivalent Li positions.

The value of the A_{iso} parameter can answer an important question concerning the covalent character of the ionic bond between the nonbridging oxygen and the alkali ion. The O–Li bond strength is directly related to the models that try to explain the ionic conductivity in glasses.[29,30] Following Morton and Preston,[31] the value $A_{\mathrm{iso}}=0.5$ MHz corresponds to about 0.135% of the unpaired electron spin density at the Li $2s$ orbital. This means that the Li–O bond is essentially ionic. Andersson and Suart have proposed a model[32] for the calculation of the activation energy required for the alkali ion to move through the glass structure. In this model, they assumed that the deformation of the electron cloud of the nonbridging oxygen will affect the ionic character of Li–O bond. Although this assumption was retained in later modifications of the model[33] no quantitative estimation of the covalency at the Li–O bond has been reported. Here, our ESEEM data allow a reliable quantitative estimation to be made and this shows that the covalent character of the Li–O bond is negligible.

V. CONCLUSION

We show that in cases with large hyperfine anisotropy and numerous overlapping peaks, contrary to one-dimensional ESEEM, HYSCORE seems to be a promising technique for the assignment of the various couplings. However, despite the considerable resolution achieved, numerical simulations are necessary in order to avoid misinterpretation that originates from experimental artefacts or from the suppression effect. The HYSCORE technique has been applied to irradiated $(Li_2O)_{0.1}(SiO_2)_{0.9}$ glass and detailed structural information was derived concerning the Li cations location and the covalent character of their bonds.

ACKNOWLEDGMENTS

We thank the Greek General Secretariat for Research and Technology and European Community for funding this research under Contract No. ENET II 296. We also thank Dr. C. Trapalis for the ICP analysis.

[1] P. Höfer, A. Grupp, H. Nebenfür, and M. Mehring, J. Chem. Phys. **132**, 279 (1986).
[2] S. A. Dikanov and Y. D. Tsvetkov, *Electron Spin Echo Modulation Spectroscopy* (CRC, Boca Raton, FL, 1992).
[3] J. Jeener, Ampére International Summer School, Basko Polje, Yugoslavia, 1971.
[4] J. J. Shane, thesis, Catholic University of Nijmegen, 1993.
[5] J. J. Shane, P. Höfer, E. J. Reijerse, and E. J. De Boer, J. Magn. Reson. **99**, 596 (1992).
[6] S. A. Dikanov and M. B. Bowman, J. Magn. Reson., Ser. A **116**, 125 (1995).
[7] P. Höfer, J. Magn. Reson., Ser. A **111**, 77 (1994).
[8] S. A. Dikanov, L. Xun, A. B. Karpiel, A. M. Tyryshkin, and M. K. Bowman, J. Am. Chem. Soc. **118**, 8408 (1996).
[9] Y. Deligiannakis and A. W. Rutherford, J. Am. Chem. Soc. **119**, 4471 (1997).
[10] B. Clotilde, T. Matsui, and J. Zimmermann, Biochemistry **35**, 14281 (1996).
[11] E. J. Reijers, J. Shane, E. De Boehr, P. Höfer, and D. Collison, Proceedings on Electron Magnetic Reasonance in Disordered systems, Gjulechita, Bulgaria, June 1991 (unpublished).
[12] S. G. Dikanov, I. R. Samoilova, A. J. Smieja, and M. K. Bowman, J. Am. Ceram. Soc. **117**, 10579 (1995).
[13] I. R. Samailova, A. S. Dikanov, V. A. Fionov, and K. M. Bowman, J. Am. Ceram. Soc. **117**, 10579 (1995).
[14] I. R. Samailova, A. S. Dikanov, V. A. Fionov, M. A. Tyryshkin, V. E. Lunina, and K. M. Bowman, J. Phys. Chem. **100**, 17621 (1996).
[15] A. Pöppl and L. Kevan, J. Phys. Chem. **100**, 3387 (1996).
[16] D. L. Griscom, J. Non-Cryst. Solids **13**, 251 (1973).
[17] T. A. Sidorov *et al.*, Teor. Eksp. Khim. **4**, 6 (1968).
[18] J. W. H. Schreuers, J. Chem. Phys. **47**, 818 (1978).
[19] D. L. Griscom, J. Non-Cryst. Solids **31**, 241 (1978).
[20] G. Kordas, B. Kamara, and H. J. Oel, J. Non-Cryst. Solids **50**, 79 (1982).
[21] J. M. Fauth, A. Schweiger, L. Braunschweiler, J. Forrer, and R. Ernst, J. Magn. Reson. **66**, 64 (1986).
[22] G. Gemperle, G. Aebli, A. Schweiger, and R. R. Ernst, J. Magn. Reson. **88**, 241 (1990).
[23] A. Abragam and B. Bleaney, *Electron Paramagnetic Reasonance of Transition Ions* (Clarendon, Oxford, 1970).
[24] K. Matar and D. Goldfarb, J. Chem. Phys. **96**, 6464 (1992).
[25] A. Ponti, J. Magn. Reson. **127**, 87 (1997).
[26] A. Dietzel, Z. Elektrochem. **48**, 9 (1942); A. C. Hannon, B. Vessal, and J. M. Parker, J. Non-Cryst. Solids **150**, 97 (1992).
[27] G. Kordas and H. J. Oel, Phys. Chem. Glasses **23**, 179 (1982).
[28] R. F. Charles, J. Am. Ceram. Soc. **45**, 105 (1962).
[29] D. E. Day, J. Non-Cryst. Solids **21**, 343 (1976).
[30] M. D. Ingram, Phys. Chem. Glasses **28**, 215 (1987).
[31] J. Morton and K. Preston, J. Magn. Reson. **30**, 577 (1977).
[32] O. L. Anderson and D. A. Stuart, J. Am. Ceram. Soc. **37**, 573 (1954).
[33] R. M. Hakim and D. R. Uhlman, Phys. Chem. Glasses **12**, 132 (1971).